Attenuation and dispersion of surface polaritons on gratings

N. E. Glass, M. Weber, and D. L. Mills
Department of Physics, University of California, Irvine, California 92717
(Received 19 September 1983)

We present theoretical studies of the influence of a diffraction grating on the dispersion relation and lifetime of surface polaritons which propagate on a periodic metallic grating. Several issues are addressed. We compare the predictions of a perturbation-theoretic analysis with the results of a nonperturbative approach based on use of the extinction theorem. The grating-induced attenuation arises from radiative decay of the surface polariton; the radiative width of the mode is compared with the magnitude of the minigaps in the dispersion relation induced by the grating. We also compare grating-induced frequency shifts and damping rates calculated directly from the implicit dispersion relation with the width and position of reflectivity dips, as calculated from a nonperturbative treatment of the coupling of an incident photon to the grating. The effects of introducing asymmetry in the grating profile are also explored quantitatively.

I. INTRODUCTION

There is considerable current interest in the study of the interaction of electromagnetic radiation with a metal surface upon which a diffraction grating is ruled. For many years,[1] it has been known that a grating may lead to resonant coupling of an incident photon to surface polaritons which propagate on the metal,[2] if the geometry is chosen so certain kinematical conditions are met. The recent interest in the topic stems from the observation that when an incident photon is coupled to a surface polariton, the strength of the electromagnetic fields near the metal surface is enhanced very substantially, when compared to those realized near a perfectly smooth surface of the same material. A consequence is that a variety of optical interactions which occur on or near the surface proceed with cross sections very much larger than can be realized on a smooth surface. An example is provided by the Raman spectroscopy of adsorbates, where it is argued[3] that the cross section scales as the fourth power of the field at the site of the molecule of interest. Very similar field enhancements may occur near protrusions on rough surfaces.[4] The diffraction grating allows the experimental study of optical interactions on surfaces of nonplanar form, under conditions where the surface profile is well characterized, and at the same time the periodic structure may more easily be subjected to theoretical analysis than a rough surface, which may contain features of substantial size and of random character.

Since it is the surface polariton which plays the key role as an intermediate state in enhanced optical couplings mediated by gratings, its intrinsic properties are clearly of fundamental interest. This paper is devoted to a study of the influence of a grating on the properties of surface polaritons. Several issues provide motivation for the analysis. First of all, in recent theoretical studies of enhanced fields near a model grating, we found[5] that as the groove depth is increased, the strength of the field first increases, but then saturates and finally decreases with increasing depth. Similar results were found by Numata,[6] and by Neviere and Reinisch,[7] who examined the theory of enhanced fields near gratings with either the profile or the spatial period different from that explored in our work.[8] We suggested in Ref. 5 that the saturation phenomenon has its origin in grating-induced radiative damping of the surface polariton. It is seen in these theoretical studies that as one increases the grating amplitude, the peak in field intensity (as a function of incidence angle or frequency), which coincides with the reflectivity dip, increases in strength as the reflectivity dip decreases, reaches its maximum value when the reflectivity dip reaches its minimum value, and then decreases as the reflectivity becomes shallower and broader. Some years ago, the behavior of the reflectivity dip as a function of grating amplitude h was itself carefully studied experimentally by Pockrand, Raether, and others.[9–12] These authors showed how the width of the reflectivity dip increases proportionally to h^2, due to the increase in the grating-induced radiative damping of the surface polariton, to which the incident light couples (in quantitative agreement with the perturbation theory of Kröger and Kretschmann[13] and the exact method of Maystre,[14] in the case of Ag, and with the method of Rosengart and Pockrand[15] for Au). Poakrand[9] and Raether[12] pointed out that the reflectivity dip reaches its smallest value for that value of h at which the radiative damping matches the dissipative losses in the material. The grating-induced radiative damping of the surface polariton should thus play a crucial role in the enhancement phenomena: the matching condition provides the optimum coupling of incident light and hence the maximum in the surface field. We should therefore like to explore the grating-damping of surface polaritons and, of course, their frequencies and wave vectors as shifted by the grating. We wish to do this directly from an exactly derived dispersion relation (whose solution for complex wave vector or complex frequency yields the damping from its imaginary part), and not just indirectly from calculated reflectivity dips nor from perturbation theory. The method that we employ is based on Green's theorem in its extinction theorem form.

Previous theoretical analyses have tended to focus on the properties of the surface polaritons at a few fixed frequencies ω and wave vectors $\vec{k}$, corresponding to those realized in certain experiments (e.g., Refs. 10 and 12). These have been at positions $(\omega,\vec{k})$ in the Brillouin zone (introduced by the grating periodicity) that are not close to the zone boundaries. We now wish to explore a larger portion of the surface-polariton dispersion curve, across several Brillouin zones, and in particular to explore the regions around the frequency gaps at the zone boundaries themselves.

These so-called "minigap" regions are of fundamental interest because the coupling between the grating and surface polariton is particularly strong there and the dispersion curves are more severely perturbed. Such band gaps are also of some technological interest because of their wave-slowing and filtering properties. A recent experimental study of surface polariton minigaps for Ag gratings was made by Chen *et al.*[16] Here we examine not only the absolute magnitude of the minigaps generated by a grating, but also their size relative to the widths of the surface polaritons. If radiative damping is sufficiently severe that the width in frequency of the surface polariton resonance is comparable to or larger than the minigap, then the latter may not be observable.

In implementing the theory numerically we have chosen to study gratings with sawtooth profiles. We are thus able to consider easily the effect, on the surface polariton frequencies and damping, of skewing the profile continuously from symmetric to asymmetric. This change in profile is seen to have a great effect on the minigap widths.

Throughout the course of the analysis presented here, we have compared the complex solutions of the dispersion relation to the calculated positions and widths of the reflectivity dips. It is the latter, in the case of fixed frequency and varying angle of incidence, for example, that the experimentalist uses as a measure of the wave vector and inverse attenuation length of the mode. It is not, however, obvious *a priori* that this procedure is valid: to employ language used in other contexts, one is in a regime where multiple scattering can lead to a variety of interference effects, which would shift the reflectivity minimum away from the renormalized frequency of the surface mode. For the example we have explored, however, we find that the solutions of the dispersion relation coincide fairly well with the reflectivity minima and widths (though this procedure is not without ambiguity, at the zone boundaries, where solutions of the dispersion relation depend on whether one uses complex ω and real k or complex k and real ω).

Finally, we have explored the range of validity of perturbation theory as a means of describing the grating-induced frequency shifts and radiative damping rates. Despite the success of Pockrand and Raether,[10,12] for example, in applying the Kröger-Kretschmann perturbation theory to their experimental reflectivity data on the shift and broadening of the dips, with Ag gratings, it is not obvious that a perturbation approach will work, even for shallow corrugations, in all circumstances, e.g., everywhere on the surface-polariton dispersion curve, including the zone boundary regions, or for different materials, or different grating profiles like the asymmetric sawtooth. For example, Raether showed that the Kröger-Kretschmann theory works much less well for Au than for Ag.[12] It is clear, moreover, that perturbation theory can fail to describe properly both the reflectivity dips and the enhanced fields near resonance, even for extremely small grating amplitudes: It is inappropriate for calculating these quantities in the observed cases for which the reflectivity from Ag gratings fall from over 90% to near zero[17] and the field intensities reach enhancements as great as 500 (Refs. 5–7 and 18) for corrugation strengths (one-half the peak-to-valley distance divided by the period) of only 0.02–0.04. On the other hand, the instances in which perturbation theory has worked well are those where the perturbed quantities being calculated are very small, like the wave-vector shift, far from any Brillouin-zone boundaries and for small amplitude sinusoidal gratings. We can thus, legitimately, question the validity of the perturbation theory for calculating the shifts and the damping of surface polaritons near zone boundaries, for asymmetric sawtooth gratings, and for corrugation strengths greater than those previously considered. We have cast the perturbation theoretic formulas into a simple and useable expression for the (complex) frequency, which is valid both at and away from the zone boundaries; and we have compared the numerical results of this expression to those of the exact methods (which itself is valid for a certain range of groove depths for which convergent results obtain).

The paper is organized as follows. In Sec. II we present a brief summary of the extinction theorem approach to deriving the dispersion relation and we outline how perturbation theory leads from this exact dispersion relation to a simple, lowest-order, expression. In Sec. III we present the results of our numerical studies and discuss their implications.

II. THE DISPERSION RELATIONS

A. The exact, extinction-theorem, formulations

The physical system that we consider (Fig. 1) consists of an isotropic dielectric medium that fills the lower half-space $x_3 < \zeta(x_1)$ and is characterized by a complex dielectric constant $\epsilon(\omega)$. The upper half-space $x_3 > \zeta(x_1)$ is vacuum. The surface profile function $\zeta(x_1)$ is periodic in x_1 with a period a (i.e., forming a classical grating). Later, in the numerical implementation of the theory, we shall focus our attention on the sawtooth profile.

A theory of the scattering of p-polarized light (i.e., transverse magnetic with respect to the plane of incidence—here $\overline{x_1 x_3}$) incident upon such a grating surface was presented by Toigo *et al.*[19] using the extinction theorem.[20] When the incident wave amplitude in this theory is set equal to zero, then a homogeneous equation results, for which the solvability condition yields the dispersion relation. The theory has been described now in

complete detail in several articles,[5,19,21,22] and will not be reproduced here. A brief outline of the theory will, however, help to define the notation.

The only nonvanishing component of the magnetic field, the x_2 component, is a function of x_1 and x_3 and is written as $H_2^{>}(x_1,x_3\,|\,\omega)e^{-i\omega t}$ in the vacuum and $H_2^{<}(x_1,x_3\,|\,\omega)^{-i\omega t}$ in the medium. Green's theorem may be written as

$$\int_\Sigma \left[G(\vec{x},\vec{x}\,')\frac{\partial H_2(\vec{x}\,')}{\partial n'} - H_2(\vec{x}\,')\frac{\partial G(\vec{x},\vec{x}\,')}{\partial n'} \right] d^2x' = \begin{cases} H_2(\vec{x}), & \vec{x}\in V \quad (2.1a) \\ 0, & \vec{x}\notin V \quad (2.1b) \end{cases}$$

where the surface Σ bounds the volume V. We first choose V to coincide with the vacuum region $x_3' > \zeta(x_1')$; then G is the well-known electromagnetic Green's function for an infinite vacuum (with radiation boundary conditions at infinity), H_2 is $H_2^{>}$, and the surface integral reduces to an integral over just the interface $x_3' = \zeta(x_1')$, with $\partial/\partial n'$ being the normal derivative (directed into the medium) at the interface. We choose the field point $\vec{x}$ with $x_3 < \zeta_{\min}$, so that the right-hand side is zero (extinction theorem). Next we choose V to be the dielectric medium; then G is the Green's function for the medium, H_2 is $H_2^{<}$, and again the integral reduces to one over the interface (and $\partial/\partial n'$ changes sign). Using the boundary conditions at the interface, we can replace $H^{<}$ by $H^{>}$ and $\epsilon^{-1}\partial H_2^{<}/\partial n$ by $\partial H_2^{>}/\partial n$. We choose $x_3 > \zeta_{\max}$ and get the extinction theorem. At this point we have two homogeneous integral equations for the two unknown functions

$$H(x_1\,|\,\omega) = H_2^{>}(x_1,x_3\,|\,\omega)\,|_{x_3=\zeta(x_1)} \quad (2.2a)$$

and

$$L(x_1\,|\,\omega) = \left[1+\left[\frac{\partial\zeta}{\partial x_1}\right]^2\right]^{1/2}\frac{\partial}{\partial n} \times H_2^{>}(x_1,x_3\,|\,\omega)\,|_{x_3=\zeta(x_1)}\,, \quad (2.2b)$$

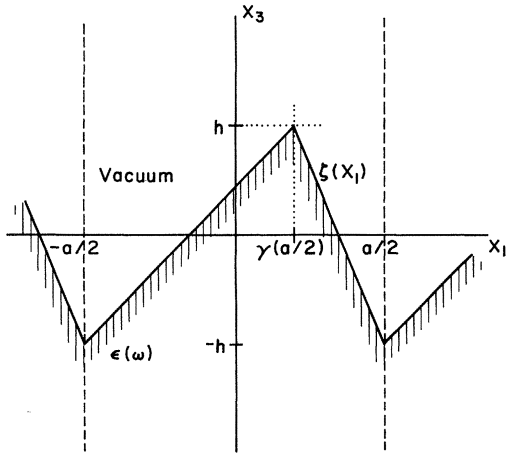

FIG. 1. Asymmetric sawtooth grating on a semi-infinite silver medium, characterized by dielectric constant $\epsilon(\omega)$, with vacuum in the upper half-space. The grating period is a and amplitude h; the asymmetry parameter is γ.

where

$$\frac{\partial}{\partial n} = \left[1+\left[\frac{\partial\zeta}{\partial x_1}\right]^2\right]^{-1/2}\left[-\frac{\partial\zeta}{\partial x_1}\frac{\partial}{\partial x_1}+\frac{\partial}{\partial x_3}\right]. \quad (2.3)$$

The integral equations are solved by expanding the unknown functions in Fourier series,

$$H(x_1\,|\,\omega) = \sum_{n=-\infty}^{\infty} e^{ik_n x_1}\hat{H}_n(k,\omega)\,, \quad (2.4a)$$

$$L(x_1\,|\,\omega) = \sum_{n=-\infty}^{\infty} e^{ik_n x_1}\hat{L}_n(k,\omega)\,, \quad (2.4b)$$

where

$$k_n = k + \frac{2\pi}{a}n\,, \quad (2.5)$$

in order to project out a set of algebraic equations:

$$\sum_{n=-\infty}^{\infty} I_{m-n}(\alpha_m(k,\omega))\left[\frac{k_m k_n-\omega^2/c^2}{\alpha_m(k\omega)}\hat{H}_n(k,\omega) + \hat{L}_n(k,\omega)\right]=0\,, \quad (2.6a)$$

$$\sum_{n=-\infty}^{\infty} I_{m-n}(-\beta_m(k,\omega))\left[\frac{k_m k_n-\epsilon(\omega)\omega^2/c^2}{\epsilon(\omega)\beta_m(k,\omega)}\hat{H}_n(k,\omega) - \hat{L}_n(k,\omega)\right]=0\,. \quad (2.6b)$$

Here we have used the following definitions:

$$I_n(\alpha_m'(k,\omega)) = \frac{1}{a}\int_{-a/2}^{a/2} dx_1 e^{-i(2\pi n/a)x_1} e^{-\alpha_m'(k,\omega)\zeta(x_1)}\,, \quad (2.7)$$

$$\alpha_m(k,\omega) = \begin{cases} (k_m^2-\omega^2/c^2)^{1/2} & \text{for } k_m^2 > \omega^2/c^2 \quad (2.8a) \\ -i(\omega^2/c^2-k_m^2)^{1/2} & \text{for } k_m^2 < \omega^2/c^2\,, \quad (2.8b) \end{cases}$$

and

$$\beta_m(k,\omega) = [k_m^2-\epsilon(\omega)\omega^2/c^2]^{1/2},\ \ \mathrm{Im}\beta_m(k,\omega) < 0\,. \quad (2.9)$$

The doubly infinite set of homogeneous linear equations for $\hat{H}_n(k,\omega)$ and $\hat{L}_n(k,\omega)$ will have solutions provided that the determinant of the coefficients vanishes. This

determinantal equation for k and ω provides the dispersion relation for the surface polaritons in the presence of a grating.

By solving Eqs. (2.6) to obtain the field and its normal derivative on the interface and by using these results in Eq. (2.1a), one can calculate the field. In the vacuum, above the selvedge region, the field is properly given by the Rayleigh sum

$$H_2^>(x_1,x_3\,|\,\omega)=\sum_{n=-\infty}^{\infty}A_n(k,\omega)e^{ik_nx_1-\alpha_nx_3}\ . \tag{2.10}$$

It is interesting to note that the Rayleigh method, whereby the Rayleigh sums for $H_2^>$ and $H_2^<$ are continued into the selvedge region to satisfy the boundary conditions, yields a set of algebraic equations for which the matrix of coefficients (for symmetric profiles) is just the transpose of that in Eqs. (2.6).[19,22] It therefore gives the same determinantal equation for the dispersion relation.

In that part of the $k\omega$ plane where $k_m^2>\omega^2/c^2$ for all m, all α_m are real and positive, so that the field is localized to the surface. The surface polariton on a grating is here a well-defined, infinitely long-lived, excitation. The dispersion curves resulting from Eqs. (2.6), for this so-called nonradiative region, were explored by Laks *et al.*[21] In the present work, we explore the radiative region of the $k\omega$ plane, where $k_m^2<\omega^2/c^2$ for one or more values of m. In this case we see from Eq. (2.8b) that one or more component waves in Eq. (2.10) represent outward radiation into the vacuum. Since energy is thus leaving the surface wave, the surface polariton is no longer a well-defined eigenmode, but instead has a finite lifetime. This leaky surface polariton should hence be described by a complex ω and/or k: we should search for zeros of the determinantal equation in the complex plane.

With complex k or ω, we must be careful about how we define the square root in Eq. (2.8) for the complex decay constant α_m. This point has been discussed in the literature for various kinds of leaky surface waves and leaky wave-guide modes. A full discussion for leaky surface elastic waves, for example, is given in Ref. 23, which we summarize here for the analogous case of surface electromagetic waves.

Consider first the case of complex ω:

$$\omega=\omega_R-i\omega_I\ , \tag{2.11}$$

where $\omega_R>0$ and where we must have $\omega_I>0$ to have a surface wave that decays in time. From Eqs. (2.11) and (2.8) we have

$$\alpha_m^2=[(k+2\pi m/a)^2-(\omega_R^2-\omega_I^2)/c^2]+i(2\omega_R\omega_I/c^2)\ , \tag{2.12}$$

so that α_m^2 must be in either the first or second quadrant of the complex plane. If we were to choose the branch-cut on the negative real axis, then α_m would always be in the first quadrant. Then α_m has a positive imaginary part, which means that the component wave (m) is traveling inward from the vacuum to the surface, opposite in direction from what is required. On the other hand, if we choose the branch-cut along the positive imaginary axis, then whenever $k_m^2<(\omega_R^2-\omega_I^2)/c^2$, putting α_m^2 in the second quadrant, the α_m will be in the third quadrant. The negative imaginary part of α_m means that the wave is now correctly radiating outwardly from the surface; the negative real part means that it is growing exponentially with distance from the surface, a necessary condition for leaky waves. That leaky waves must always have a seeming divergence at $x_3=\infty$ was discussed by Ingebrigtsen and Tonning,[24] who pointed out that the usual radiation boundary condition of finite amplitudes at $x_3=\infty$ is not applicable. A divergence at $x_3=\infty$ at time t can develop only for a wave that leaves the surface at $t=-\infty$ (since the wave needs infinite time to reach $x_3=\infty$), but then the surface wave itself has an infinite amplitude, due to its exponential form $e^{-\omega_I t}$. Thus there is a divergence at $x_3=+\infty$ because of the built-in divergence at $t=-\infty$: leaky waves are not normalizable. In a real physical situation, the surface excitation is begun at some time, say $t=0$, and then after a finite time t, the wave leaking out from the surface cannot have traveled farther than ct; so that for $x_3>ct$ there is no wave and hence no divergence. That an exponential increase with distance into the vacuum is physically correct, a necessary consequence of the finite speed of propagation, can be seen clearly by writing a component of $H_2^>$ [from the sum in Eq. (2.10)] for which $k_m^2<(\omega_R^2-\omega_I^2)/c^2$, and hence $\alpha_m=-|\alpha_R|-i|\alpha_I|$, namely,

$$\begin{aligned}[H_2^>(x_1,x_3\,|\,\omega)]_m e^{-i\omega t_0}&=\exp\{-\omega_I[t_0-x_3/(\omega_I/|\alpha_R|)]\}A_m\exp[i(k_mx_1+|\alpha_I|x_3-\omega_Rt_0)]\\&\propto A_{\rm surf}(t=t_0-x_3/\tilde{c})A_m\exp[i(k_mx_1+|\alpha_I|x_3-\omega_Rt_0)]\ ,\end{aligned} \tag{2.13}$$

where $\tilde{c}\equiv\omega_I/|\alpha_R|$. At time t_0, this component wavelet m represents an outgoing plane wave with an amplitude that is proportional to the amplitude on the surface at the *retarded time* $t=t_0-x_3/\tilde{c}$ when the wavelet left the surface.

In the case of complex k,

$$k=k_R+ik_I\ , \tag{2.14}$$

k_R may be positive or negative, and k_I must have the same sign as the group velocity (in an extended zone scheme, k_I will have the same sign as k_R). Then we have

$$\alpha_m^2=[(k_R+2\pi m/a)^2-k_I^2-\omega^2/c^2]+i[2(k_R+2\pi m/a)k_I]\ . \tag{2.15}$$

From Eq. (2.15), it can be seen that only the choice of branch-cut along the positive imaginary axis will lead to outgoing radiated waves in the vacuum, with nonzero am-

plitude at $x_3=\infty$. Again, there is an exponential increase with distance into the vacuum, and that this is physically correct is shown by an argument analogous to the one just presented for complex ω (see Ref. 23).

Before turning to a discussion of the numerical results of the exact dispersion relation, arising from Eqs. (2.6), we first show how perturbation theory applied to that set of equations leads to a simple and useful expression.

B. Perturbation theory

Various formulations of perturbation theory have been presented, to treat the scattering of light from rough (especially randomly rough) planar surfaces, in the limit that the roughness amplitude is small. These theories have also been applied to gratings and to the properties of surface polaritons on gratings. In particular, the work of Kröger and Kretschmann[13] was employed by Pockrand and Raether[10] and by Raether[12] in a comparison to their experimental work on light scattering from gratings. The positions and widths of the measured reflectivity minimum, as a function of grating amplitude, corresponding to two points ωk *within* a Brillouin zone (defined by the grating periodicity) were compared to the theory (quite successfully for Ag, and somewhat less so for Au). Toigo *et al.*,[19] by expanding Eq. (2.7) to first order in $\alpha\zeta$, showed how the extinction theorem result leads to a dispersion relation; then, in the case of a grating, they solved for the dispersion relation at a Brillouin-zone boundary in the two beam approximation (i.e., keeping only the terms with $k=\pm n\pi/a$). At about the same time, one of us[25] explored the minigaps as a function of the angle between the wave vector of the surface polariton, and the grating grooves. This was also done within the two-beam approximation, and with use of the Rayleigh hypothesis. One may demonstrate that the results of Ref. 25 and those in Ref. 19 are in agreement.

In the perturbation theory described here, we begin with the extinction theorem results and derive a simple algebraic expression for the dispersion relation, keeping *all* terms to first order in $\alpha\zeta$. We take into account the effect of the nonresonant terms in Eq. (2.6) by solving for the corresponding L_n and H_n in terms of all of the grating modes. Since the contribution from the resonant terms will be most important, we can thus write the nonresonant L_n and H_n in terms of the resonant modes. This procedure leads to a simple eigenvalue equation which yields the dispersion relation valid to first order in the grating height.

We begin by expanding the integral in Eq. (2.7) to first order in ζ,

$$I_{m-n}(\alpha_m(k,\omega))=\delta_{m-n,0}-\zeta_{m-n}\alpha_m \ , \tag{2.16a}$$

$$I_{m-n}(-\beta_m(k,\omega))=\delta_{m-n,0}+\zeta_{m-n}\beta_m \ , \tag{2.16b}$$

where

$$\zeta_{m-n}=\frac{1}{a}\int_{-a/2}^{a/2}dx_1 e^{-i(2\pi/a)(m-n)x_1}\zeta(x_1) \ . \tag{2.17}$$

Thus ζ_m is the mth Fourier component of the surface profile function $\zeta(x_1)$. Note that $\zeta_0=0$ by construction. Inserting into Eq. (2.6) we find an expression relating one mode to all the rest:

$$L_m+\alpha_m H_m=\sum_{n=-\infty}^{\infty}\zeta_{m-n}\alpha_m\left[L_n+\frac{H_n}{\alpha_m}\left[k_m k_n-\frac{\omega^2}{c^2}\right]\right], \tag{2.18a}$$

$$\epsilon L_m-\beta_m H_m = -\sum_{n=-\infty}^{\infty}\zeta_{m-n}\beta_m\left[\epsilon L_n-\frac{H_n}{\beta_m}\left[k_m k_n-\epsilon\frac{\omega^2}{c^2}\right]\right] . \tag{2.18b}$$

These equations can be solved for L_m and H_m to yield

$$L_m=\sum_n\frac{\zeta_{m-n}}{\epsilon\alpha_m+\beta_m}[\Lambda_{11}(m,n)L_n+\Lambda_{12}(m,n)H_n] \ , \tag{2.19a}$$

$$H_m=\sum_n\frac{\zeta_{m-n}}{\epsilon\alpha_m+\beta_m}[\Lambda_{21}(m,n)L_n+\Lambda_{22}(m,n)H_n] \ , \tag{2.19b}$$

where

$$\begin{aligned}\Lambda_{11}(m,n)&=\alpha_m\beta_m(1-\epsilon) \ ,\\ \Lambda_{12}(m,n)&=(\alpha_m+\beta_m)k_m k_n-(\epsilon\alpha_m+\beta_m)\frac{\omega^2}{c^2} \ ,\\ \Lambda_{21}(m,n)&=\epsilon(\alpha_m+\beta_m) \ ,\\ \Lambda_{22}(m,n)&=k_m k_n(\epsilon-1) \ .\end{aligned} \tag{2.20}$$

Let ω_{m_1},k_{m_1} correspond to a surface polariton in the absence of the grating. Now, suppose that we examine a mode with wave vector k_{m_1} near a zone boundary. There will exist a mode with wave vector $k_{m_2}=k_{m_1}-(m_1-m_2)2\pi/a$ which will be coupled strongly by the grating to the k_{m_1} mode. This coupling will manifest itself through the vanishing of the denominators, to zeroth order, of the form $\epsilon\alpha_{m_1}+\beta_{m_1}$ and $\epsilon\alpha_{m_2}+\beta_{m_2}$, thereby causing L_{m_1}, H_{m_1}, L_{m_2}, and H_{m_2} to become large.

We can rewrite the above equations for $m=m_1$, pulling the large resonant terms out of the sum:

$$L_{m_1}=\frac{\zeta_{m_1-m_2}}{\epsilon\alpha_{m_1}+\beta_{m_1}}[\Lambda_{11}(m_1,m_2)L_{m_2}+\Lambda_{12}(m_1,m_2)H_{m_2}]+\sum_{n\,(\neq m_2)}\frac{\zeta_{m_1-n}}{\epsilon\alpha_{m_1}+\beta_{m_1}}[\Lambda_{11}(m_1,n)L_n+\Lambda_{12}(m_1,n)H_n] \ , \tag{2.21a}$$

$$H_{m_1}=\frac{\zeta_{m_1-m_2}}{\epsilon\alpha_{m_1}+\beta_{m_1}}[\Lambda_{21}(m_1,m_2)L_{m_2}+\Lambda_{22}(m_1,m_2)H_{m_2}]+\sum_{n\,(\neq m_2)}\frac{\zeta_{m_1-n}}{\epsilon\alpha_{m_1}+\beta_{m_1}}[\Lambda_{21}(m_1,n)L_n+\Lambda_{22}(m_1,n)H_n] \ . \tag{2.21b}$$

Similar expressions can be written for L_{m_2} and H_{m_2}. Now, we can approximate the Λ's, when $m=m_1$ or $m=m_2$, by their zeroth-order values where $\epsilon\alpha_{m_{1,2}}+\beta_{m_{1,2}}=0$:

$$\begin{aligned}\Lambda_{11}(m,n)&=\epsilon(\epsilon-1)\alpha_m^2\ ,\\ \Lambda_{12}(m,n)&=-(\epsilon-1)\alpha_m k_m k_n\ ,\\ \Lambda_{21}(m,n)&=-\epsilon(\epsilon-1)\alpha_m\ ,\\ \Lambda_{22}(m,n)&=k_m k_n(\epsilon-1)\ .\end{aligned}\tag{2.22}$$

Inserting these expressions in Eq. (2.21), we see that $L_{m_1}=-\alpha_{m_1}H_{m_1}$ and $L_{m_2}=-\alpha_{m_2}H_{m_2}$. Putting the above relationship for the resonant terms into Eq. (2.21) and into the related equations for L_{m_2} and H_{m_2}, we find

$$\begin{aligned}H_{m_1}=&\frac{\zeta_{m_1-m_2}(\epsilon-1)}{\epsilon\alpha_{m_1}+\beta_{m_1}}(k_{m_1}k_{m_2}+\epsilon\alpha_{m_1}\alpha_{m_2})H_{m_2}\\&+\sum_{n\,(\neq m_2)}\frac{\zeta_{m_1-n}(\epsilon-1)}{\epsilon\alpha_{m_1}+\beta_{m_1}}(k_{m_1}k_nH_n-\epsilon\alpha_{m_2}L_n)\ .\end{aligned}\tag{2.23}$$

A similar expression holds for H_{m_2}, with m_1 and m_2 interchanged. If we multiply the H_{m_1} equation by $\epsilon^2\alpha_{m_1}^2-\beta_{m_1}^2$, then we will be able to obtain an eigenvalue equation for ω. Note that

$$\epsilon^2\alpha_{m_1}^2-\beta_{m_1}^2=\frac{\epsilon(\epsilon-1)}{c^2}(\omega_{m_1}^2-\omega^2)\ ,\tag{2.24}$$

where

$$\omega_{m_1}^2=c^2k_{m_1}^2\frac{\epsilon+1}{\epsilon}$$

is just the unperturbed frequency of a surface polariton of wave vector k_{m_1}. The equation for H_{m_1} becomes, after setting $\epsilon\alpha_{m_1}+\beta_{m_1}=0$ on the right-hand side and rearranging,

$$\omega^2H_{m_1}=\omega_{m_1}^2H_{m_1}-\Delta(m_1,m_2)H_{m_2}-\sum_{n\,(\neq m_2)}[V_a(m_1,n)H_n+V_b(m_1,n)L_n]\ ,\tag{2.25a}$$

and the H_{m_2} equation analogously becomes

$$\omega^2H_{m_2}=\omega_{m_2}^2H_{m_2}-\Delta(m_2,m_1)H_{m_1}-\sum_{n\,(\neq m_1)}[V_a(m_2,n)H_n+V_b(m_2,n)L_n]\ ,\tag{2.25b}$$

where we have substituted

$$\Delta(m_1,m_2)=2c^2\alpha_{m_1}(k_{m_1}k_{m_2}+\epsilon\alpha_{m_1}\alpha_{m_2})\zeta_{m_1-m_2}\ ,\tag{2.26}$$

$$V_a(m_1,n)=2c^2\alpha_{m_1}k_{m_1}k_n\zeta_{m_1-n}\ ,\tag{2.27}$$

$$V_b(m_1,n)=-2c^2\epsilon\alpha_{m_1}^2\zeta_{m_1-n}\ .\tag{2.28}$$

Now, we can approximate the nonresonant L_n and H_n in Eq. (2.25) by only the resonant contribution from Eq. (2.19); that is, by

$$L_n=\sum_{i=1,2}\frac{\zeta_{n-m_i}}{\epsilon\alpha_n+\beta_n}V_c(n,m_i)\ ,\tag{2.29a}$$

$$H_n=\sum_{i=1,2}\frac{\zeta_{n-m_i}}{\epsilon\alpha_n+\beta_n}V_d(n,m_i)\ ,\tag{2.29b}$$

where

$$V_c(n,m_i)=\zeta_{n,m_i}\left[(\alpha_n+\beta_n)k_nk_{m_i}+(\epsilon-1)\alpha_n\beta_n\alpha_{m_i}-(\epsilon\alpha_n+\beta_n)\frac{\omega^2}{c^2}\right]\ ,\tag{2.30}$$

$$V_d(n,m_i)=\zeta_{n-m_i}[k_nk_{m_i}(\epsilon-1)-\epsilon(\alpha_n+\beta_n)\alpha_{m_i}]\ .\tag{2.31}$$

We insert Eq. (2.29) into Eq. (2.25) to obtain

$$\omega^2H_{m_1}=\tilde{\omega}_{m_1}^2H_{m_1}-\tilde{\Delta}(m_1,m_2)H_{m_2}\ ,\tag{2.32a}$$

$$\omega^2H_{m_2}=\tilde{\omega}_{m_2}^2H_{m_2}-\tilde{\Delta}(m_2,m_1)H_{m_1}\ ,\tag{2.32b}$$

where

$$\tilde{\Delta}(m_i,m_j)=\Delta(m_i,m_j)+\sum_{n\,(\neq m_i,m_j)}\frac{V_a(m_i,n)V_d(n,m_j)+V_b(m_i,n)V_c(n,m_j)}{\epsilon\alpha_n+\beta_n}\tag{2.33}$$

are the effective coupling constants, renormalized by the grating, and

$$\tilde{\omega}_{m_i}^2=\omega_{m_i}^2-\sum_{n\,(\neq m_i,m_j)}\frac{V_a(m_i,n)V_d(n,m_i)+V_b(m_i,n)V_c(n,m_i)}{\epsilon\alpha_n+\beta_n}\tag{2.34}$$

are the renormalized versions of the unperturbed frequencies. By inspection, one can pick out the eigenvalues from (2.32) to be

$$\omega_\pm^2=\tfrac{1}{2}(\tilde{\omega}_{m_1}^2+\tilde{\omega}_{m_2}^2)\pm\tfrac{1}{2}[(\tilde{\omega}_{m_1}^2-\tilde{\omega}_{m_2}^2)^2+4\tilde{\Delta}(m_1,m_2)\tilde{\Delta}(m_2,m_1)]^{1/2}\tag{2.35}$$

This simple algebraic expression is to first order in the grating height the dispersion relation for surface polaritons on a grating. It can be used away from the gaps to give the dispersion curve in the near vicinity of the Brillouin-zone boundary. As one moves aways from the zone boundary, to the point where $|\tilde{\omega}_{m_1}^2-\tilde{\omega}_{m_2}^2|^2>4\tilde{\Delta}(m_1,m_2)\tilde{\Delta}(m_2,m_1)$, then the square root in Eq. (2.35) may be expanded. Then if in the term $\pm\tilde{\Delta}(m_1,m_2)\tilde{\Delta}(m_2,m_1)/(\tilde{\omega}_{m_1}^2-\tilde{\omega}_{m_2}^2)$ generated by this

procedure one retains only the lowest-order contribution in the grating amplitude (replace $\tilde{\Delta}$ by Δ and $\tilde{\omega}$ by ω), one may show that the renormalized frequencies are then given by $\tilde{\omega}^2_{m_1}$ and $\tilde{\omega}^2_{m_2}$ as defined in Eq. (2.34), with the restriction $n \neq m_j$ removed. Now when the restriction $n \neq m_j$ is removed from the right-hand side of Eq. (2.34), the resulting form is precisely the expression for the *complex* frequency shift of the mode provided by second-order perturbation theory. Recall that the imaginary part has its origin in radiation-induced radiation damping. Thus, as we move away from the gap, Eq. (2.35) evolves into an expression identical to that produced by second-order perturbation theory, applied away from the zone boundary. This equivalence holds so long as one does not stray too far from the zone boundary.

By using the nonresonant terms to renormalize the unperturbed frequencies, of the interacting waves m_1 and m_2, as described in Eq. (2.34), we obtain, at the Brillouin-zone boundaries, shifts in the gap-center frequencies which are not present in the two-beam approximation. Moreover, since the nonresonant terms include the modes which radiate into the vacuum, their presence is required to provide a description of the leaky surface polariton lifetime.

III. NUMERICAL RESULTS

In this section we shall consider the numerical solution, in the complex plane, of the exact dispersion relation from Eq. (2.6) and of the perturbation theory relation, Eq. (2.35). The surface profile function chosen is the sawtooth profile, of amplitude h (one-half the peak-to-valley distance) and with deviation from a symmetric profile measured by γ (see Fig. 1):

$$\zeta(x_1)=\begin{cases}\dfrac{4x_1h/a+(1-\gamma)h}{1+\gamma}, & -\dfrac{a}{2}\le x_1\le\gamma\dfrac{a}{2}\\[2ex] \dfrac{-4x_1h/a+(1+\gamma)h}{1-\gamma}, & \gamma\dfrac{a}{2}\le x_1\le\dfrac{a}{2}\end{cases} \tag{3.1}$$

which is repeated in every cell. For this profile we have that

$$I_n(\alpha)=\frac{4\alpha h e^{-i(\pi/2)\gamma n}}{\pi^2n^2+(2\alpha h+i\pi n\gamma)^2} \times\begin{cases}\sinh(\alpha h+i\pi\gamma n/2), & n \text{ even}\\ -\cosh(\alpha h+i\pi\gamma n/2), & n \text{ odd}.\end{cases} \tag{3.2}$$

Most of the work reported here is for Ag, in which case the grating period is $a=8000$ Å; and the values of the complex dielectric constant $\epsilon(\omega)$ are taken or extrapolated from the table in Ref. 26. We have also briefly considered the case of Au, for which we have taken $a=4417$ Å and $\epsilon=-6.8+i1.81$ to conform with the work of Raether.

The zeros of the infinite dimensional determinant of the coefficients of the unknowns in Eq. (2.6) are found by solving the N-dimensional determinantal equation $[m,n=-(N/2-1)/2,\ldots,0,\ldots,(N/2-1)/2$ in Eq. (2.6)] and then searching for convergence as N is increased. The convergence of the results is much faster for $\gamma=0$ (symmetric grating) than for $\gamma\neq0$, and is progressively slower as the corrugation strength (h/a) is increased. It is generally slower as we move up the dispersion curve, i.e., as k and ω are increased, and is also much slower in the case of Au than Ag.

For Ag ($a=8000$ Å) at $h=300$ Å ($h/a=0.0375$) convergence is very rapid, even for quite large values of γ: for example, at $\gamma=0.35$ for k up to $1.5(2\pi/a)$, four-figure accuracy in ω_R and in ω_I is achieved with $N=26$. It is only for $\gamma>0.9$ that convergence becomes difficult at this amplitude. At $h=800$ Å, for $\gamma=0$, convergence to within a few meV or better can be achieved [with $N=20$ at $k=1.5(2\pi/a)$, but with $N=62$ at other nearby values of k]. For $\gamma\neq0$ and this same h, however, the convergence achieved is poorer. For $\gamma=0$, we have gone up to $h=1600$ Å ($h/a=0.2$), for which we find, at the zone boundary $k=1.5(2\pi/a)$, that four-figure accuracy for ω_R and about three figures for ω_I is achieved at $N=66$.

Convergence in the case of Au is more difficult: even with just $h=300$ Å ($a=4417$ Å), there are oscillations in the fourth figure of k_R until $N>82$, and not until $N\approx102$ do we approach four-figure accuracy.

For the symmetric Ag grating, we show a comparison in Table I of the results of the exact theory with the perturbation theory, for the two complex frequencies $\omega_R^{(-)}-i\omega_I^{(-)}$ and $\omega_R^{(+)}-i\omega_I^{(+)}$ at the Brillouin-zone boundary $k=1.5(2\pi/a)$. Even for the largest value of h (1600 Å), the perturbation theory is within 1% of the exact theory for the real parts of the frequency. Agreement is fairly good for the imaginary part of the upper-branch mode, $\omega_I^{(+)}$, at least up to 800 Å. It is only for $\omega_I^{(-)}$, the damping of the lower-branch zone-boundary mode (the mode most strongly perturbed, as seen by the bending of the dispersion curve) that the results begin to agree poorly already at $h=800$ Å. But on moving away from the zone boundary to smaller values of k, while remaining on the same branch of the dispersion curve, the agreement in ω_I immediately improves [15% error in ω_I at $k=1.3(2\pi/a)$ rather than the 26% at $1.5(2\pi/a)$, for $h=800$ Å]. Table I also shows the width in frequency of the boundary modes as a percentage of the gap width, indicating that this gap should be observable at $h=300$ Å but not at $h=800$ Å.

In Fig. 2, for the symmetric sawtooth grating with $h=300$ Å, we have plotted the dispersion curve, from $k\lesssim2\pi/a$ to $k\gtrsim1.5(2\pi/a)$, as obtained from the exact dispersion relation for complex ω and real k and also for complex k and real ω, the perturbation theory, and the reflectivity minima. The corresponding imaginary parts of the solutions, ω_I and k_I, and the reflectivity widths are shown in Fig. 3. The reflectivity calculations (using the method of Ref. 5), for the widths in Fig. 3, are of two kinds. (1) We fix the incident photon frequency ω and vary the angle of incidence θ and hence vary $k_0=(\omega/c)\sin\theta$; this corresponds to solving the dispersion relation for complex k, where k_I should give the half-width at half maximum of the dip in reflectivity versus k_0. (2) We vary the incident frequency ω with fixed incidence angle. In this case both ω and k_0 are simultaneously changing, so that the correspondence between ω_I and the half-width of reflectivity versus ω is not exact; the

TABLE I. Complex frequency solutions ($\omega_R^{(-)}-i\omega_I^{(-)}$ and $\omega_R^{(+)}-i\omega_I^{(+)}$) of the dispersion relation for the two modes at the zone boundary $k=1.5(2\pi/a)$ [and one mode at $k=1.3(2\pi/a)$]—exact and perturbation (pert.) theory compared. For symmetric sawtooth gratings (period $a=8000$ Å) on Ag, with amplitudes h.

h (Å)		Energy in eV $\hbar\omega_R^{(-)}$	$\hbar\omega_I^{(-)}$	$\hbar\omega_R^{(+)}$	$\hbar\omega_I^{(+)}$	Gap width $\hbar\omega_G$ (meV)	$(\omega_I^{(-)}+\omega_I^{(+)})/\omega_G$
$k=1.5(2\pi/a)$							
100	exact	2.228	0.003 65	2.241	0.003 50	13	0.55
	pert.	2.231	0.003 64	2.245	0.003 40	14	
	% diff.	0.13	0.27	0.18	2.9		
300	exact	2.211	0.009 8	2.249	0.008 35	38	0.43
	pert.	2.211	0.009 3	2.253	0.008 51	42	
	% diff.	0	5.1	0.18	1.9		
800	exact	2.147	0.065 6	2.251	0.043 5	104	1.05
	pert.	2.141	0.048 8	2.256	0.044 6	115	
	% diff.	0.28	25.6	0.22	2.5		
1600	exact	1.955	0.425	2.204	0.190	249	2.47
	pert.	1.942	0.202	2.201	0.171	259	
	% diff.	0.66	52.5	0.14	10.0		
$k=1.3(2\pi/a)$							
800	exact	1.934	0.039 2				
	pert.	1.928	0.033 4				
	% diff.	0.31	14.8				

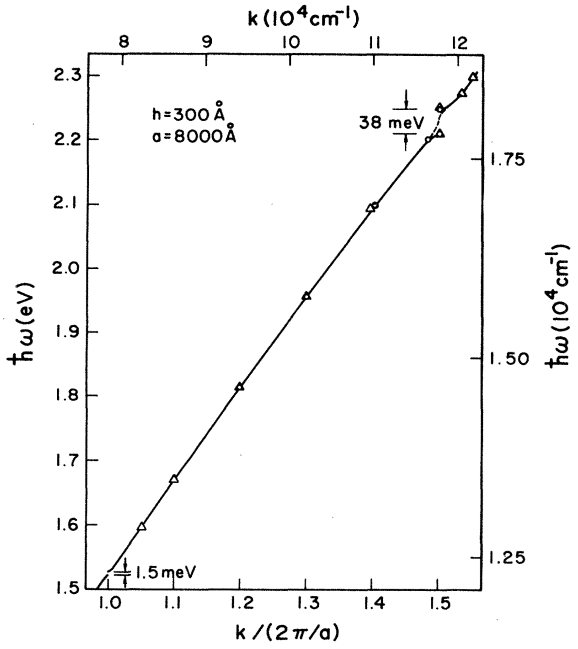

FIG. 2. Dispersion relation for surface polaritons on a symmetric sawtooth grating (amplitude $h=300$ Å, period $a=8000$ Å) on Ag. The solid and dashed lines are calculated by the exact extinction-theorem method: with complex frequency (real wave vector) and with complex wave vector (real frequency), respectively. Open circles are solutions from perturbation theory for complex frequency. Triangles shows the frequency of calculated reflectivity minima (on varying the incident photon frequency with fixed incidence angle).

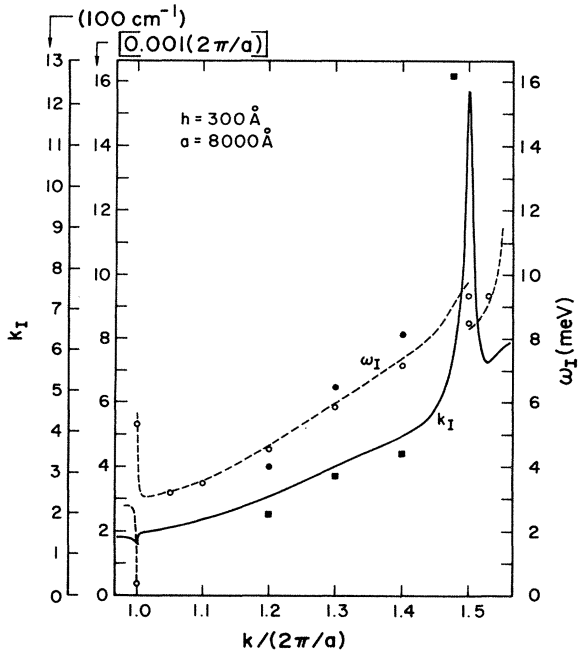

FIG. 3. Imaginary part of the complex wave-vector solution, k_I, and imaginary part of the complex frequency solution, ω_I, both vs real (or real part of) k, for surface polaritons on a symmetric sawtooth grating (amplitude $h=300$ Å) on Ag. The solid and dashed lines show the exact extinction-theorem solutions, for k_I and ω_I, respectively. Open circles show ω_I from perturbation theory. Closed circles indicate the calculated width of the dip in reflectivity-versus-incidence-frequency (fixed θ); squares show the corresponding width in reflectivity-versus-$k=(\omega/c)\sin\theta$, on varying θ (fixed ω).

resonant surface polariton here has wave vector $k_1=(\omega/c)\sin\theta+2\pi/a$; on varying ω by $\Delta\omega$, we have

$$\Delta k_1/k_1=\frac{\Delta\omega}{\omega}\left[1+\left[k_0\Big/\frac{2\pi}{a}\right]\right]^{-1}\ll\frac{\Delta\omega}{\omega},$$

and hence the correspondence between ω_I and half-width is not bad.

The four methods are in agreement on the dispersion curve in Fig. 2, except that right near the zone boundary $k=1.5(2\pi/a)$, the exact solution for complex k deviates slightly from the other solutions. For complex k there are solutions (heavily damped) right across the frequency gap. Correspondingly, the reflectivity with constant ω shows a very shallow dip, as a function of θ, in this "gap" region. Nevertheless, the reflectivity calculation for constant θ does give two completely distinct dips at $k=1.5(2\pi/a)$, i.e., the gap is observable in that sense.

The agreement between perturbation theory and the exact theory for ω_I (Fig. 3) is good. The agreement between the exact theory for ω_I or k_I and the corresponding half-widths of reflectivity-versus-ω (constant θ) or reflectivity-versus-θ (constant ω) is just slightly poorer (better for k_I than ω_I, as expected).

Note that since the reflectivity curves are sometimes broad and shallow, the frequency, wave vector, and damping obtained from their positions and widths are not always as precisely determined as they are from the other calculations. Moreover, in the present case, a surface polariton with $k\approx 2\pi/a$ is at a point on the dispersion curve near the light line, so that the corresponding reflectivity dip at $\theta\approx 0°$ is very close to a Wood's threshold anomaly, which we have seen can severely distort the shape of the resonance dip. Then it is impossible to determine the polariton lifetime from the width of the reflectivity dip.

Between the two zone boundaries, $1.0\leq k/(2\pi/a)<1.5$, we see $\hbar\omega_I$ vary between approximately 3 and 10 meV (while $\hbar\omega_R$ varies between about 1.5 and 2.2 eV), corresponding to lifetimes from 1.38×10^{-12} sec down to 0.416×10^{-12} sec. Here k_I is about 120 cm^{-1} at $k_R=1.0(2\pi/a)$ and then sharply peaks up past 1200 cm^{-1} at $k_R=1.5(2\pi/a)$—corresponding to an attenuation length, $1/2k_I$, of 4.2×10^{-3} to 4.2×10^{-4} cm.

As the zone boundary at $k=1.0(2\pi/a)$ is approached along the upper branch of the dispersion curve, i.e., from larger to smaller k, the frequency width ω_I of the mode turns upward and increases rapidly (see Fig. 3), up to 5.53 meV. As the gap there is only 1.5 meV, it is totally washed out by the width of the upper mode. Notice that this gap at $k=1.0(2\pi/a)$ is much narrower than that at $k=1.5(2\pi/a)$. In fact, there is no gap at all at $k=1.0(2\pi/a)$ in the two-beam approximation of lowest-order perturbation theory, for the symmetric sawtooth grating (or for any profile that is symmetric about $x=0$ and at the same time antisymmetric about $x=a/4$), because $\zeta_{\pm2}=0$. This being the case, it is interesting to consider the effect, on this "forbidden gap" at $k=1.0(2\pi/a)$, of increasing γ from 0 to 1, that is, of making the grating asymmetrical. In Fig. 4 (again for $h=300$ Å) we have plotted the real parts of the frequencies of the upper and lower zone-boundary modes, as a function of γ, for

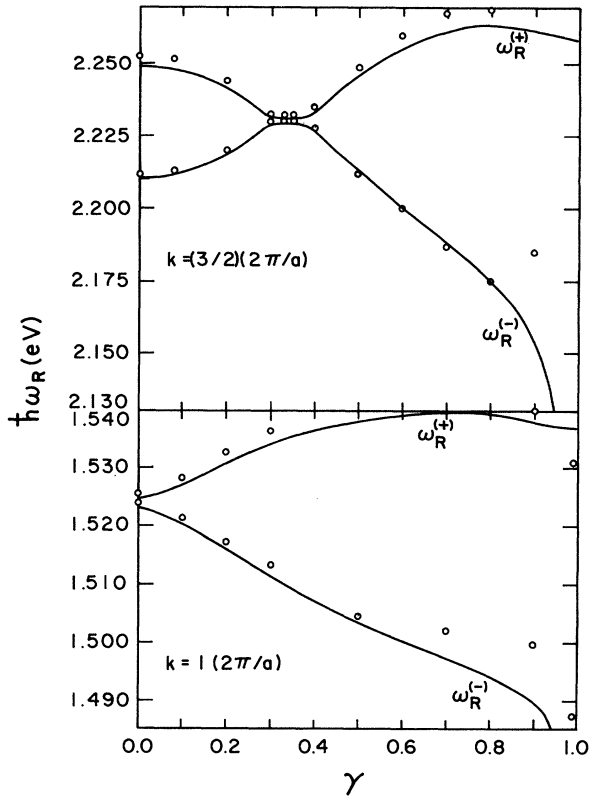

FIG. 4. Real parts of the complex frequencies for the two surface-polariton modes ($\omega_R^{(-)}$ and $\omega_R^{(+)}$) at the zone boundary $k=1(2\pi/a)$ (bottom) and at the boundary $k=1.5(2\pi/a)$ (top), plotted vs the asymmetry parameter γ, for a sawtooth grating ($h=300$ Å, $a=8000$ Å) on Ag. The solid line is from the exact extinction-theorem method; the circles are from perturbation theory.

$k=1(2\pi/a)$ and also $k=1.5(2\pi/a)$. In Fig. 5 are the corresponding imaginary parts ω_I. Note that the perturbation theory works well, except for the larger values of γ, e.g., $\gamma>0.8$. For $\gamma>0.9$ the values of $\omega_R^{(-)}$ and of $\omega_I^{(-)}$ both begin to increase in a divergent manner as $\gamma\to1.0$. In this same range of γ, the convergence of the results, as a function of matrix size N, becomes more and more difficult, and we stop calculating $\omega^{(-)}$ at $\gamma=0.96$.

We see from Fig. 6, for $k=1.0(2\pi/a)$, that the gap width increases continually with increasing γ: the gap increases from 1.5 meV to about 50 meV at $\gamma=0.9$. At the same time, as also seen in Fig. 6, the sum of the half-widths of the two modes, $\omega_I^{(-)}+\omega_I^{(+)}$, is fairly constant with changing γ: the sum just decreases from 5.89 to 5.08 meV, as γ goes from 0.0 to 0.8, and then increases slightly to 5.85 meV, as γ reaches 0.9 (before beginning its divergence as $\gamma\to1$). Thus the ratio of gap width to mode linewidth is continuously increasing with γ. The gap is already wider than the sum of the mode half-widths when γ reaches 0.1 and is almost nine times wider when $\gamma=0.8$.

The situation for the gap at $k=1.5(2\pi/a)$ is different. Here the gap width is seen (Figs. 4. and 6) to decrease at first with increasing γ ($\gamma=0$–0.3) and then to increase (for $\gamma>0.4$). Again, the sum $\omega_I^{(-)}+\omega_I^{(+)}$ is fairly constant out to near $\gamma=0.9$. It is only between $\gamma=0.2$ and

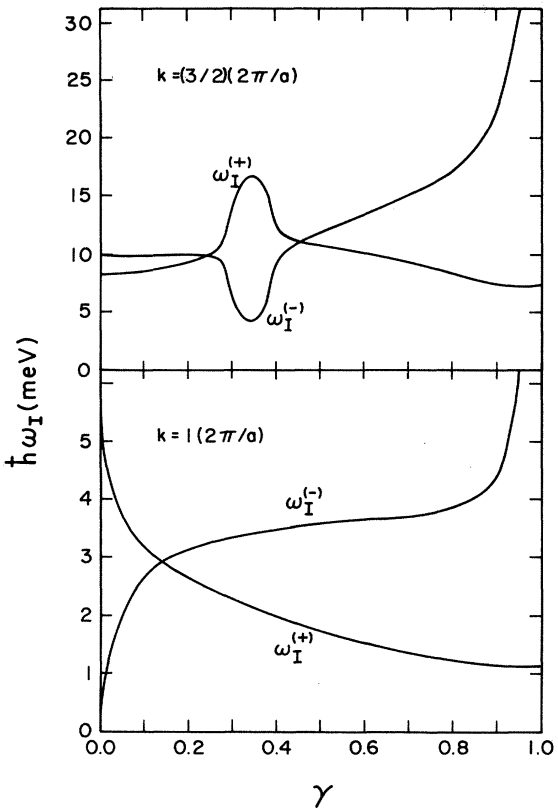

FIG. 5. Imaginary parts of the complex frequencies for the two surface-polariton modes ($\omega_I^{(-)}$ and $\omega_I^{(+)}$) at the zone boundary $k=1(2\pi/a)$ (bottom) and at the boundary $k=1.5(2\pi/a)$ (top), plotted vs the asymmetry parameter γ, for a sawtooth grating ($h=300$ Å, $a=8000$ Å) on Ag.

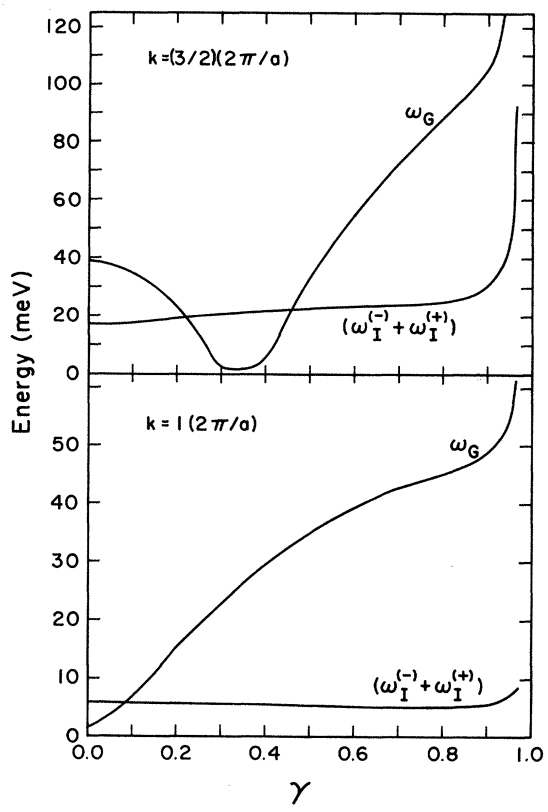

FIG. 6. Frequency gap ω_G and also the sum of the imaginary parts of the frequencies of the two surface polaritons ($\omega_I^{(-)}+\omega_I^{(+)}$) at the zone boundary $k=1(2\pi/a)$ (bottom) and at the boundary $k=1.5(2\pi/a)$ (top), plotted vs the asymmetry parameter γ, for a sawtooth grating ($h=300$ Å, $a=8000$ Å) on Ag.

0.46 where the gap width is smaller than the sum of the two line half-widths.

In Fig. 7 we show the surface polariton dispersion curve for a symmetric grating of amplitude $h=800$ Å and period $a=8000$ Å on Ag, as determined from solving the exact dispersion relation for complex ω. The corresponding imaginary part of the solution, ω_I, is plotted in Fig. 8 as a function of the real frequency ω_R. The grating amplitude at this point is beyond where the extinction theorem method of Ref. 5 for the reflectivity gives convergent results. Notice that, even in this $\gamma=0$ case, the gap at $k=1.5(2\pi/a)$ is now over 100 meV wide, and even the "forbidden gap" at $k=1.0(2\pi/a)$ is 25 meV wide.

IV. CONCLUSIONS

We have shown that numerical solutions of the dispersion relation, which result from application of the extinction theorem, may be found in the complex plane for leaky surface polaritons on a metallic grating surface. Thus we are able to calculate both the dispersion and attenuation (lifetime or attenuation length) of surface polaritons in the radiative region of the (k,ω) plane. Convergence of the solutions is found for symmetric gratings of large amplitude (far beyond where the Rayleigh hypothesis is suppose to break down, even though the extinction theorem leads to the same dispersion relation for symmetric gratings as does the Rayleigh method), and convergence is also found for asymmetric gratings. We have carried out most of our calculations for Ag gratings; we have also explored gratings of Au, and found the convergence more difficult to achieve for Au than for Ag.

These solutions provide a more direct indication of the dispersion and lifetime of the surface modes than does the position and width of the reflectivity dip, the latter possibly being subject to interference effects. Although there is generally good agreement between our solutions of the dispersion relation and the results from our calculations of the reflectivity dips, we have indeed seen cases where the latter are difficult to decipher: where there is heavy damping of the surface polariton and the reflectivity minimum becomes broad and shallow and where, in the case of a nearby Wood's threshold anomaly, the reflectivity dip is highly asymmetric and distorted. Furthermore, we can obtain convergent results for the solutions of the dispersion relation far beyond where convergence breaks down ($h\approx 600$ Å and $a=8000$ Å for Ag) in the corresponding extinction-theorem calculation of the reflectivity.

A perturbation theory applied to the dispersion relation, in which we keep the nonresonant as well as resonant terms, yields a simple dispersion relation valid in the radiative region, at—as well as away from—the Brillouin-zone boundaries. Its complex solutions, in the case of Ag,

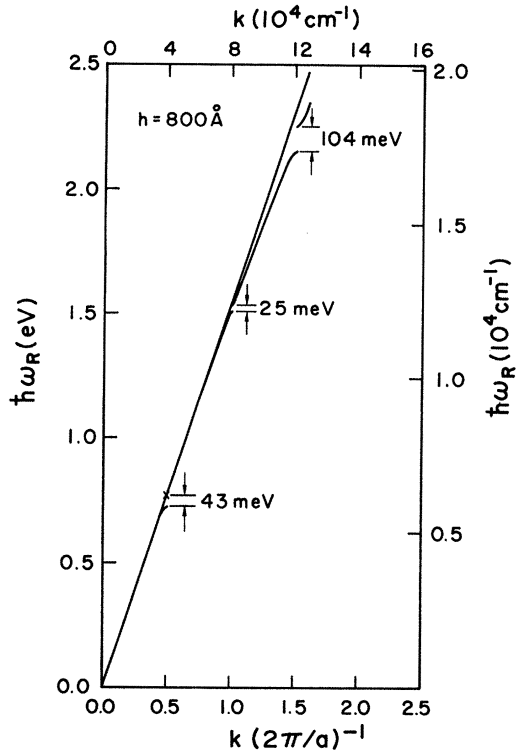

FIG. 7. Dispersion relation for surface polaritons on a symmetric sawtooth grating ($h=800$ Å, $a=8000$ Å) on Ag. Calculated by the exact extinction-theorem method, with complex frequency and real wave vector.

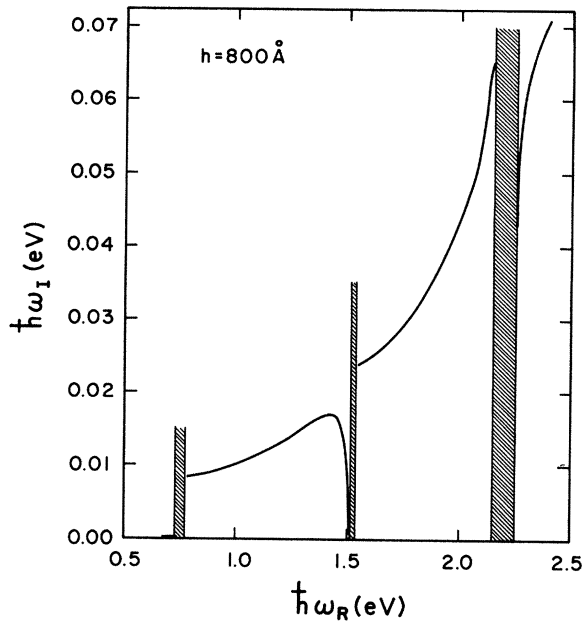

FIG. 8. Imaginary part vs the real part of the complex frequency, calculated by the exact extinction-theorem method, for surface polaritons on a symmetric sawtooth grating ($h=800$ Å, $a=8000$ Å) on Ag. Shaded regions are the band gaps.

agree well with those of the exact theory, for asymmetric as well as symmetric profiles, and for large corrugation strengths (far beyond those at which the reflectivity dip reaches its minimum value and the field enhancements reach their maximum): even at $h=1600$ Å, there is less than 1% deviation in the real parts, i.e., in the dispersion. In fact, we stopped our comparative calculation of the dispersion at $h=1600$ Å because of convergence difficulties (i.e., larger and larger necessary matrix size) in the exact theory and not because of breakdown in the perturbation theory. This points out an important conclusion of this work, namely, the advantage of using the perturbation theory over the exact theory, for a broad range of physical parameters. The exact theory, involving a search in the complex plane for the solution of a complex, large-dimensional, determinantal equation, is highly consuming in both human and computer time. Complex root finding subroutines are not capable of zeroing in on these solutions without a good initial guess (to almost three figures in the real and imaginary parts) and thus a tedious on-line search is necessary to begin the procedure. Furthermore, convergence of the exact solutions is a problem; it must be checked at almost every point (k,ω), for every set of parameters (h,a,γ): Too small a matrix and the results oscillate with N, too big a matrix and divergences set in. On the other hand, the perturbation theory can be implemented on a hand calculator.

As for the physical results, we have seen how the grating-induced radiative damping of the surface polaritons can totally obscure a zone-boundary minigap or may have little effect on the gap—depending on which zone boundary is involved and on, of course, the grating amplitude. Both the gap width and the damping widths of the zone-boundary modes are very strongly affected by the degree of asymmetry (measured by our parameter γ) in the surface profile. The properties of a minigap can, in principal, be controlled.

As remarked in Sec. I, Raether found it difficult to account for his measured grating-induced dispersion relation shifts on Au gratings,[12] while the perturbation theory proved quantitatively adequate for Ag. We have been unable to locate the origin of the discrepancy.

ACKNOWLEDGMENT

This research was supported by U.S. National Aeronautics and Space Administration (NASA), through Contract No. NAG3-250.

[1]U. Fano, J. Opt. Soc. Am. 31, 213 (1941).

[2]See, for example, the collection of articles in *Surface Polaritons*, edited by V. M. Agranovich and D. L. Mills (North-Holland, Amsterdam, 1982).

[3]See, for example, the articles in *Surface Enhanced Raman Scattering*, edited by R. K. Chang and T. E. Furtak (Plenum, New York, 1982).

[4]See, for example, R. Ruppin, Solid State Commun. 39, 903

(1981), and J. Gersten and A. Nitzan, J. Chem. Phys. 73, 3023 (1980).

[5]D. L. Mills and M. Weber, Phys. Rev. B 26, 1075 (1982); M. Weber and D. L. Mills, *ibid.* 27, 2698 (1983).

[6]H. Numata, J. Phys. Soc. Jpn. 51, 2575 91982).

[7]M. Neviere and R. Reinisch, Phys. Rev. B 26, 5403 (1982).

[8]Numata explored a grating of sinusoidal profile, with the same spatial period as we (D.L.M. and M.W.) used in Ref. 5. His results for the magnitude of the enhanced field associated with the reflectivity dip in the visible (2.6 eV), and its variation with groove depth are remarkably similar to ours. In our study, in the visible range of frequency, the grating with 8000-Å period leads to the presence of several (~ 5) Bragg beams. The structure explored by Reinisch and Neviere was analyzed only in a spectral region where no Bragg beams are present, and all diffracted waves produced by the incident photons are evanescent in character. The differences in value of the enhanced fields obtained in the two studies thus do not have their origin in the presence of a dielectric layer, as we suggested earlier (Ref. 5); instead the two studies examine very different spectral regimes. One of us (D.L.M.) is grateful to Dr. Reinisch for his comments on this point.

[9]I. Pockrand, J. Phys. D 9, 2423 (1976).

[10]I. Pockrand and H. Raether, Appl. Opt. 16, 1784 (1977).

[11]W. Rothballer, Opt. Commun. 20, 429 (1977).

[12]H. Raether, Opt. Commun. 42, 217 (1982).

[13]E. Kröger and E. Kretschmann, Phys. Status Solidi B 76, 515 (1976).

[14]D. Maystre, Opt. Commun. 8, 216 (1973).

[15]E. H. Rosengart and I. Pockrand, Opt. Lett. 1, 194 (1977).

[16]Y. J. Chen, E. S. Koteles, R. J. Seymour, G. J. Sonek, and J. M. Ballantyne, Solid State Commun. 46, 95 (1983).

[17]D. Maystre and R. Petit, Opt. Commun. 17', 196 (1976); M. C. Hutley and D. Maystre, *ibid.* 19, 431 (1976).

[18]P. Sheng, R. S. Stepleman, and P. N. Sanda, Phys. Rev. B 26, 2907 (1982).

[19]F. Toigo, A. Marvin, V. Celli, and N. R. Hill, Phys. Rev. B 15, 5618 (1977).

[20]For related usage of the extinction theorem, in studies of scattering from rough planar surfaces, earlier than Ref. 19, see: J. L. Uretsky, Ann. Phys. 33, 400 (1965); G. S. Agarwal, Opt. Commun. 14, 161 (1975); P. C. Waterman, J. Acoust. Soc. Am. 57, 791 (1975).

[21]B. Laks, D. L. Mills, and A. A. Maradudin, Phys. Rev. B 23, 4965 (1981).

[22]A. A. Maradudin, in *Surface Polaritons,* edited by V. M. Agranovich and D. L. Mills (North-Holland, Amsterdam, 1982), pp. 405—510.

[23]N. E. Glass and A. A. Maradudin, J. Appl. Phys. 54, 796 (1983).

[24]K. A. Ingebrigtsen and A. Tonning, Phys. Rev. 184, 942 (1969).

[25]D. L. Mills, Phys. Rev. B 15, 3097 (1977).

[26]P. B. Johnson and R. W. Christy, Phys. Rev. B 6, 4370 (1972).